ARL

US Army Research Laboratory

Power Spectral Density and Hilbert Transform

by Patrick Jungwirth

NOTICES

Disclaimers

The findings in this report are not to be construed as an official Department of the Army position unless so designated by other authorized documents.

Citation of manufacturer's or trade names does not constitute an official endorsement or approval of the use thereof.

Destroy this report when it is no longer needed. Do not return it to the originator.

US Army Research Laboratory

Power Spectral Density and Hilbert Transform

by Patrick Jungwirth
Computational and Information Sciences Directorate, ARL

1. REPORT DATE *(DD-MM-YYYY)*	2. REPORT TYPE	3. DATES COVERED (From - To)
December 2016	Technical Report	September 2016

4. TITLE AND SUBTITLE	5a. CONTRACT NUMBER
Power Spectral Density and Hilbert Transform	
	5b. GRANT NUMBER
	5c. PROGRAM ELEMENT NUMBER

6. AUTHOR(S)	5d. PROJECT NUMBER
Patrick Jungwirth	
	5e. TASK NUMBER
	5f. WORK UNIT NUMBER

7. PERFORMING ORGANIZATION NAME(S) AND ADDRESS(ES)	8. PERFORMING ORGANIZATION REPORT NUMBER
US Army Research Laboratory ATTN: RDRL-CIH-S Aberdeen Proving Ground, MD 21005-5067	ARL-TR-7920

9. SPONSORING/MONITORING AGENCY NAME(S) AND ADDRESS(ES)	10. SPONSOR/MONITOR'S ACRONYM(S)
	11. SPONSOR/MONITOR'S REPORT NUMBER(S)

12. DISTRIBUTION/AVAILABILITY STATEMENT

Approved for public release; distribution is unlimited.

13. SUPPLEMENTARY NOTES

14. ABSTRACT

This technical report focuses on the Hilbert transform and some of its applications for digital signal processing. Herein we review power spectral density and complex exponentials, and illustrate how the Hilbert transform converts a real signal (real in the sense of a real time domain function and symmetric Fourier transform) into an analytic signal. We then demonstrate how multiplication by a complex exponential is used for frequency translation and provide 2 uses for the Hilbert transform in a software-defined radio: 1) creating an analytic signal and 2) recovering single sideband. Examples of upgrading a software-defined radio architecture with new algorithms (software) are also provided.

15. SUBJECT TERMS

Fourier transform, Hilbert transform, digital filter, SDR

16. SECURITY CLASSIFICATION OF:			17. LIMITATION OF ABSTRACT	18. NUMBER OF PAGES	19a. NAME OF RESPONSIBLE PERSON
			UU	42	Patrick Jungwirth
a. REPORT	b. ABSTRACT	c. THIS PAGE			19b. TELEPHONE NUMBER (Include area code)
Unclassified	Unclassified	Unclassified			410-278-6174

Contents

List of Figures

1. Introduction

This report explains the key concepts used in a software-defined radio (SDR). Important concepts for SDRs are frequency and phase translation. Complex exponentials provide a convenient way to translate frequency and shift phase. Herein, we review complex numbers, power spectral density, Dirac delta function, Fourier transform, analytic functions, and the Hilbert transform.

Section 2 introduces the concepts and tools required to understand the Hilbert transform. We begin by discussing the Dirac delta function and power spectral density. Power spectral density describes how much power is contained in a narrow bandwidth, typically 1 Hz. For example, for a power spectral density of 1.3 W/Hz in a 1-Hz bandwidth, there is 1.3 W of power. How much bandwidth does a pure sine wave require? The bandwidth of an ideal sine wave is 0 Hz. How do you represent a 1-W sine wave source (power concentrated in a single frequency) on a power spectral density graph (power per frequency, watts per hertz)? The Dirac delta function is used to represent power concentrated in zero bandwidth.

Later in Section 2, we introduce the Hilbert transform by presenting examples of real signals and analytic signals. The Hilbert transform is the key step to convert a real signal to an analytic signal (function). We then present a Fourier transform proof to derive the Hilbert transform.

Section 3 covers digital signal processing for an SDR and illustrates the advantages of analytic signals, frequency translation, and phase shift.

The Appendix presents a review of complex numbers, where we start off with a simple number line for a bottom-up approach to explain the properties of complex numbers. We explain how complex numbers are built up from real numbers. In digital signal processing, the multiplication property of complex numbers (analytic functions) provides for simple frequency translation and phase shift.

2. Digital Signal Processing Introduction

This section introduces the concepts and tools required to understand the Hilbert transform. Also covered are the Dirac delta function, single-sided power spectral density, double-sided power spectral density, Fourier transform, properties of real functions, and analytic signals.

We begin by introducing the Dirac delta function and power spectral density. Power spectral density is used to explain the properties of complex exponentials and analytic functions. Analytic signals are a generalization of complex exponentials.

An analytic signal has the same frequency translation and phase shift properties as a complex exponential function.

2.1 Dirac Delta Function

The Dirac delta function is defined as the limit as the pulse's height approaches infinity, $\delta(t) = \lim_{heigth \to \infty} pulse(t)$, while the area under the pulse remains equal to 1 (Fig. 1). An arrow is used to draw the unit area Delta function on a graph. The Dirac delta function in Eq. 1 only has a nonzero value when the argument inside equals 0, when $t = t_o$. The delta function in Eq. 2 occurs at $t = -4$, and it has a height or strength of –3. The function $\delta(t + 4)$ has unit area. We draw $g(t)$ as an arrow with a height of –3 on a graph. Since the Dirac delta function has all of its area concentrated as a point, we can use the delta function to represent the power contained in a sine wave (zero bandwidth) on a power spectral density graph.
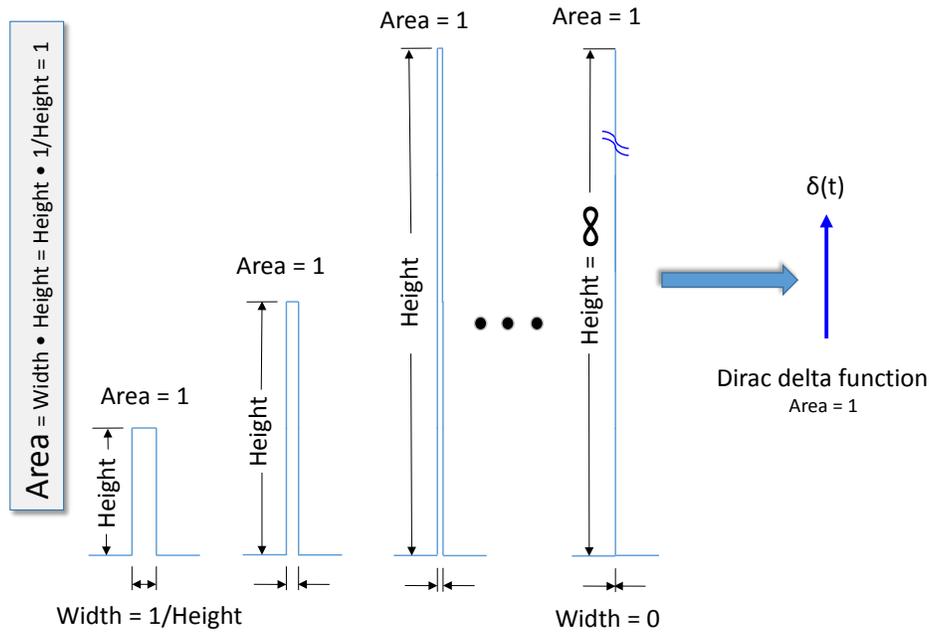
Fig. 1   Dirac delta function

$$f(t) = \delta(t - t_o) \tag{1}$$

$$g(t) = -3\delta(t + 4) \tag{2}$$

2
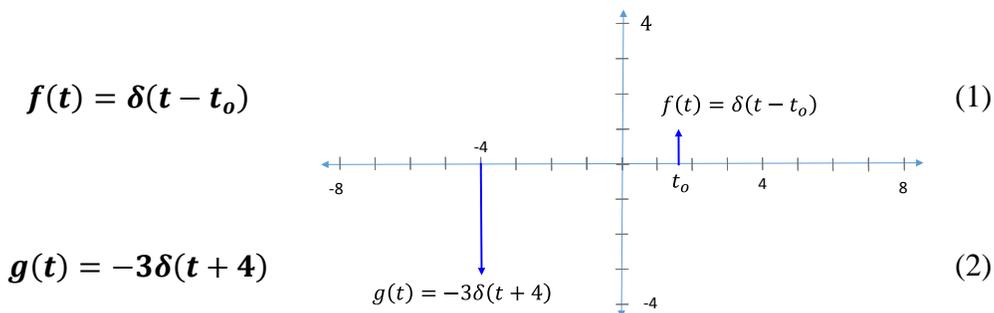
The probability distribution for a die simulation is presented in Fig 2. The probability distribution for an ideal die is 1/6 for die = 1, 2, 3, 4, 5, or 6. The simulation results are close to 1/6. The histogram in Fig. 2 shows discrete probability values. How do we represent the die values on a continuous number line? This is the same question as asking, How do we show a sine wave's power concentrated at a single frequency on a power spectral density graph? On the continuous number line, shown in Fig. 3, the die probabilities are concentrated at the points (die values) x = 1, 2, 3, 4, 5, and 6. The delta functions show the probability density concentrated at the points. We will use delta functions to show power concentrated at a single frequency on a power spectral density graph.
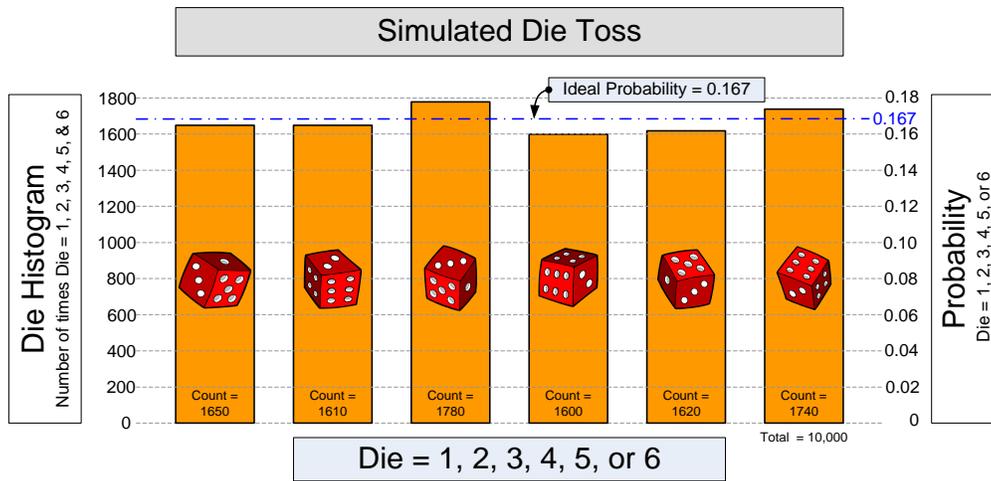
Fig. 2   Die toss simulation
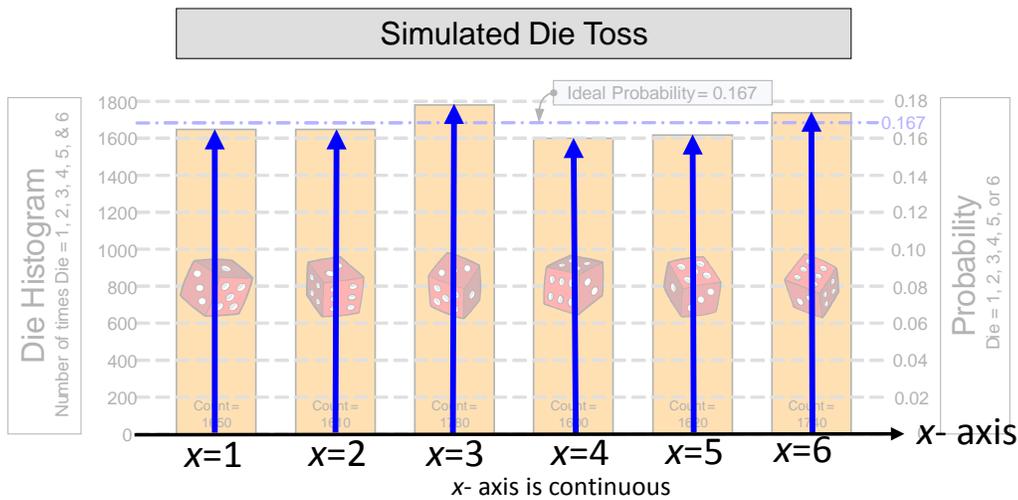
Fig. 3   Delta functions show density concentrated at a point

2.2 Fourier Transform

The Fourier transform converts a time function, $f(t)$, into the frequency domain, $F(j\omega)$, (complex exponentials) as shown in Eq. 3. The functions $f(t)$ and $F(j\omega)$ are called a Fourier transform pair. Figure 4 shows the Fourier transform squared, $|F(j\omega)|^2$, for a square wave. The unit for power spectral density is $\frac{W}{Hz}$. The unit $\frac{W}{Hz}$ tells us how much power is concentrated in a 1-Hz bandwidth. Power is voltage squared, $P = \frac{V^2}{R}$, and we generally set the resistance to $R = 1\ \Omega$, so $P = V^2$. This means that the unit for the Fourier transform is $\frac{\text{volts RMS}}{\sqrt{\text{Hz}}}$. The power spectral density is the Fourier transform squared, $|F(j\omega)|^2$. On a decibel scale, $P = 10log(P)$ dB and $P = 20log(V)$ dB. On a decibel graph, the power spectral density in terms of $\frac{W}{Hz}$ looks the same as $\frac{\text{volts RMS}}{\sqrt{\text{Hz}}}$. The only difference is the scale factor of 2 from $P = 10log(P)$ and $P = 20log(V)$.

$$f(t) = \frac{1}{2\pi} \int_{\omega=-\infty}^{+\infty} F(j\omega)e^{j\omega t}\, d\omega \quad \Longleftrightarrow \quad F(j\omega) = \int_{t=-\infty}^{+\infty} f(t)e^{-j\omega t} dt \qquad (3)$$

Fig. 4   Square wave power spectral density graph

In this report, we use double-sided power spectral density graphs. Double-sided spectra are in terms of complex exponentials. The positive and negative frequencies in Fig. 4 show how much power is present in the positive frequency terms, $e^{+j2\pi ft}$, and negative frequency terms, $e^{-j2\pi ft}$. Single-sided power spectral d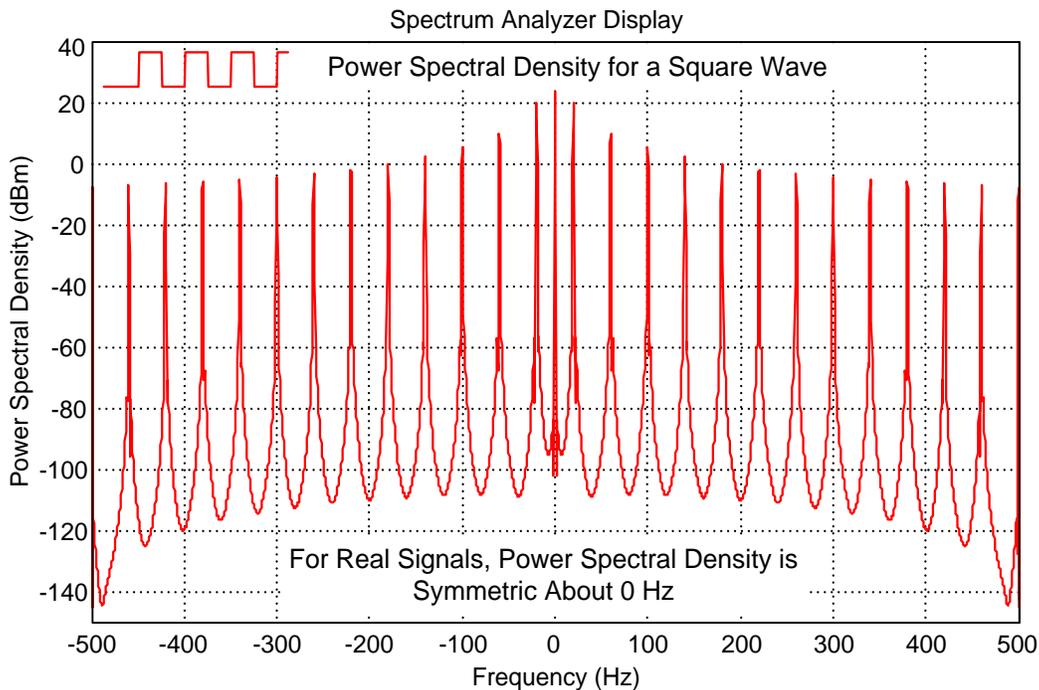ensity combines the positive, $e^{+j2\pi ft}$, and negative terms, $e^{-j2\pi ft}$, into cosines, since $cos\varphi = \frac{e^{j\varphi}+e^{-j\varphi}}{2}$. Real functions, like $cos\varphi$ and the square wave in Fig. 4, have a symmetric power spectral density graph. For real functions, the power spectral density for positive complex exponential, $e^{+j2\pi ft}$, and negative complex exponential, $e^{-j2\pi ft}$, terms are equal (graph is a mirrored image across 0 Hz). In the following section, we make use of the properties of real functions to find the Hilbert transform.

2.3 Hilbert Transform

The Hilbert transform is a math function used to convert a real function into an analytic signal (function). As illustrated in Section 2.3, an analytic signal has the same frequency and phase shift properties as a complex exponential function. We will show the advantages of using analytic signals in digital signal processing compared to real signals like $g(t) = cos(2\pi ft)$.

Figure 5 shows the frequency spectrum of the product of 2 complex exponentials. For $f(t) = e^{+j2\pi 20t}$ and $g(t) = e^{+j2\pi 30t}$, the product is $h(t) = f(t)g(t) = e^{+j2\pi 20t}e^{+j2\pi 30t}$ and $h(t) = e^{+j2\pi 50t}$. We see a single spectral line at 50 Hz.
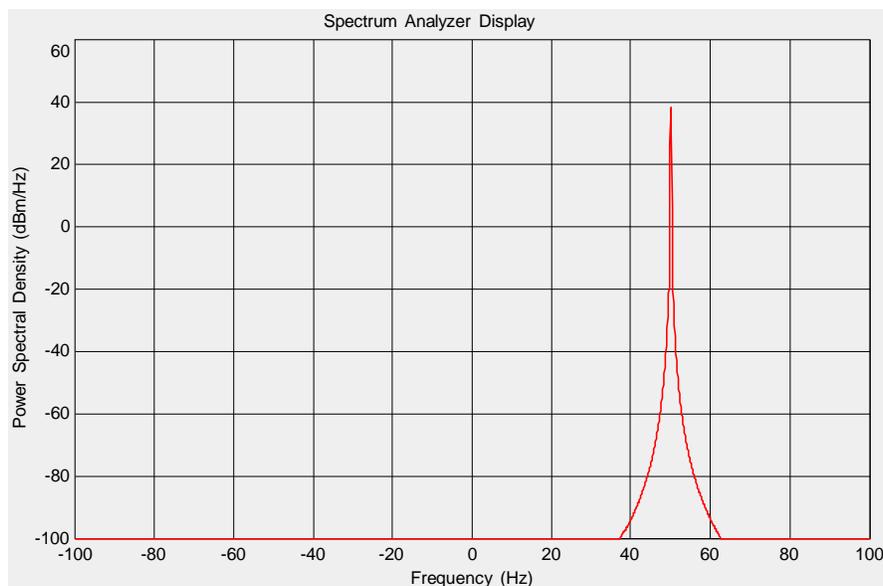
Fig. 5   **Frequency spectrum of $e^{+j2\pi 50t} = e^{+j2\pi 20t} \cdot e^{+j2\pi 30t}$**

Figure 6 shows the frequency spectrum for the product of 2 real cosine functions. For $f(t) = cos(2\pi 20t)$ and $g(t) = cos(2\pi 30t)$, the product $h(t) = f(t)g(t) = cos(2\pi 20t)cos(2\pi 30t)$. The product results in sum and difference frequencies, $f = 30 \pm 20$ Hz: $h(t) = \frac{1}{2}[cos(2\pi 50t) + cos(2\pi 10t)]$. In Fig. 6, we see 4 power spectral density terms: $cos(2\pi 50t) = \frac{1}{2}(e^{j2\pi 50t} + e^{-j2\pi 50t})$ and $cos(2\pi 10t) = \frac{1}{2}(e^{j2\pi 10t} + e^{-j2\pi 10t})$.
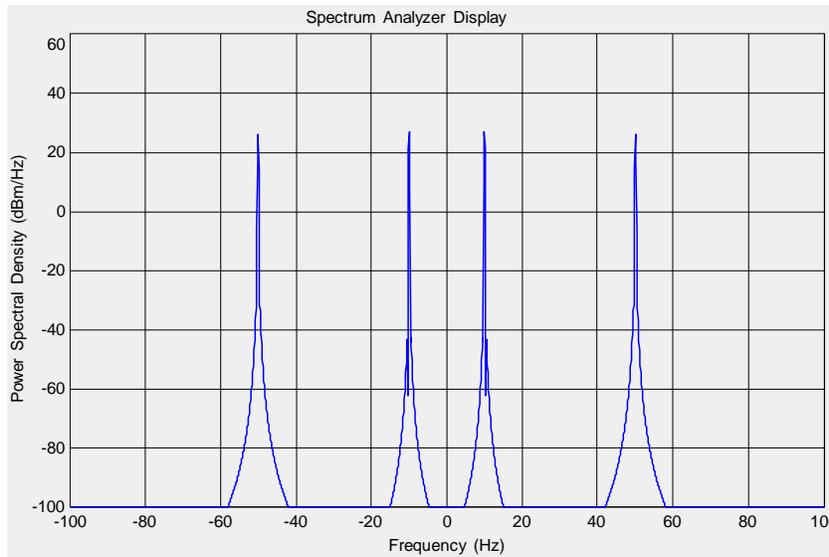
Fig. 6   **Frequency spectrum of $cos(2\pi 50t) + cos(2\pi 10t) = 2cos(2\pi 20t)cos(2\pi 30t)$**

We would like to convert $f(t) = cos(2\pi 20t)$ and $g(t) = cos(2\pi 30t)$ into complex exponentials to take advantage of the multiplication property illustrated in Fig. 5. In Fig. 5 there is only a single frequency term, whereas in Fig. 6 there are sum and difference frequency terms.

A very good approximation to the ideal Hilbert transform is a low-pass finite impulse response (FIR) filter. In Fig. 7, we show a real signal, $f(t) = cos(2\pi 20t)$, converted to an analytic signal using a 255-tap Hilbert transform low-pass filter. For an ideal Hilbert transform, there would be no signal present at –20 Hz. We then use a complex multiply to frequency translate the 20-Hz signal to 50 Hz.
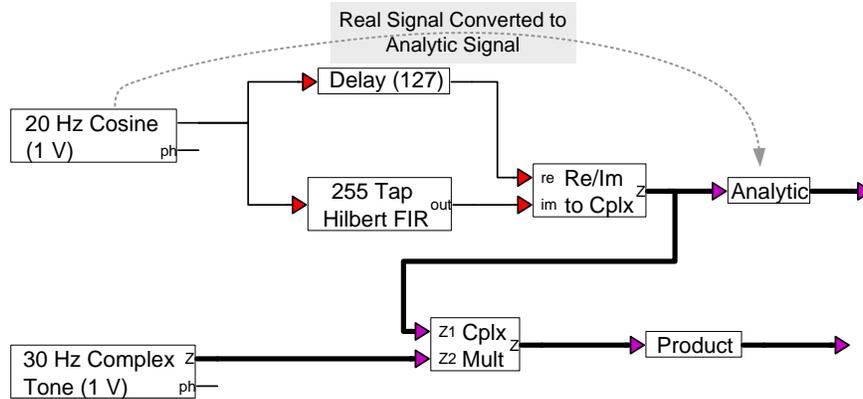
Fig. 7   Hilbert transform applied to a real signal, $cos(2\pi 20t)$, and used to convert a real signal to an analytic signal; complex multiply is then used to create a single frequency term at 20 + 30 Hz.

Figure 8 shows the 20-Hz signal frequency translated to 50 Hz, with a very small signal present at +10 Hz (–48 dBm, which is 76 dB lower than the carrier signal at +28 dBm). The power spectral density graph in Fig. 8 shows a single frequency term at 50 Hz and an insignificant term at +10 Hz.
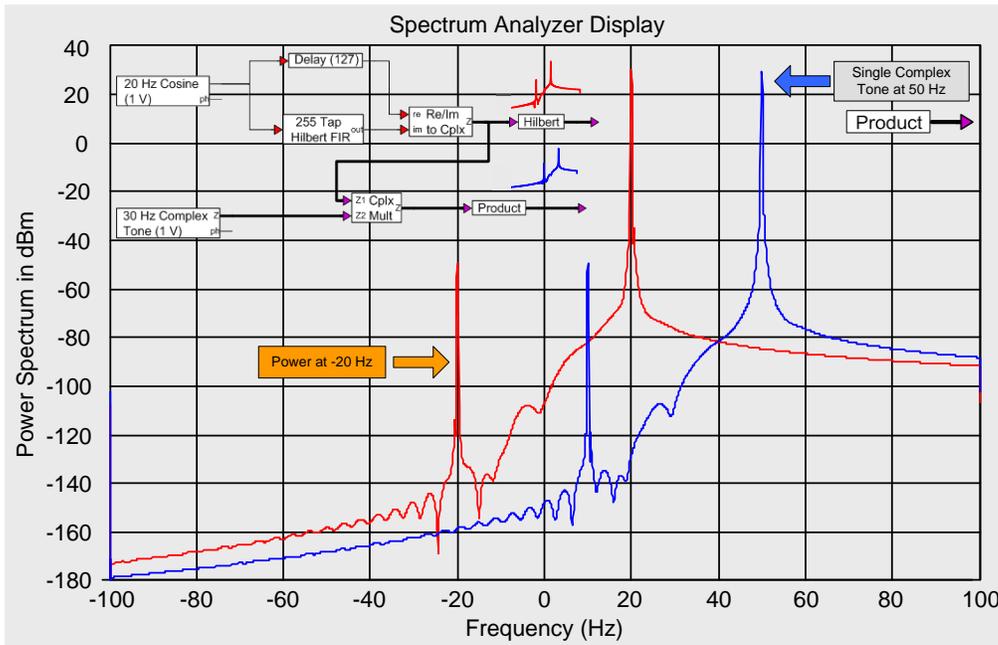
Fig. 8   Frequency spectrum from block diagram in Fig. 7 showing a single frequency term at 20 + 30 Hz

An analytic signal has only positive frequency, complex exponential terms, $e^{+j2\pi ft}$, in its power spectral density graph. Figure 8 gives an example of an analytic signal. The power spectral density for negative frequencies is so small that it can be ignored (power at –20 Hz is orders of magnitude smaller than the power present at 20 Hz).

7

We present a derivation showing how to convert a real signal to an analytic signal. An analytic signal is more general than the complex exponentials discussed previously. An analytic signal has the same frequency translation and phase shift properties as a complex exponential. We will derive the Hilbert transform filter to convert a real signal to an analytic signal. Figure 9 compares the power spectral density properties for real and analytic signals. Equations 4–9 cover the derivation for the Hilbert transform. The results are summarized in Fig. 10.

Figure 9 shows that a real signal, $R(j\omega)$, has a symmetric power spectral density. We need to find the spectrum for the analytic signal, $A(j\omega)$, which consists of only positive frequency terms. Equation 4 defines the Fourier transform pair for the real signal. A real signal has the Fourier transform property in Eq. 5. In Eq. 6, we calculate the analytic signal, $A(j\omega)$, in terms of the real signal, $R(j\omega)$. In Eq. 7, we use the unit step function to simplify Eq. 6. The sign function, or signum function, from Eq. 8 is substituted to simplify again. In Eq. 9, we use the Fourier transform pair from Eq. 8 to simply the analytic function.

Power Spectral Density

Real Signal
$R(j\omega)$

Analytic Signal
$A(j\omega)$

Real Signal or Real Function
has a symmetric power
spectral density

Negative Frequency Terms   Positive Frequency Terms
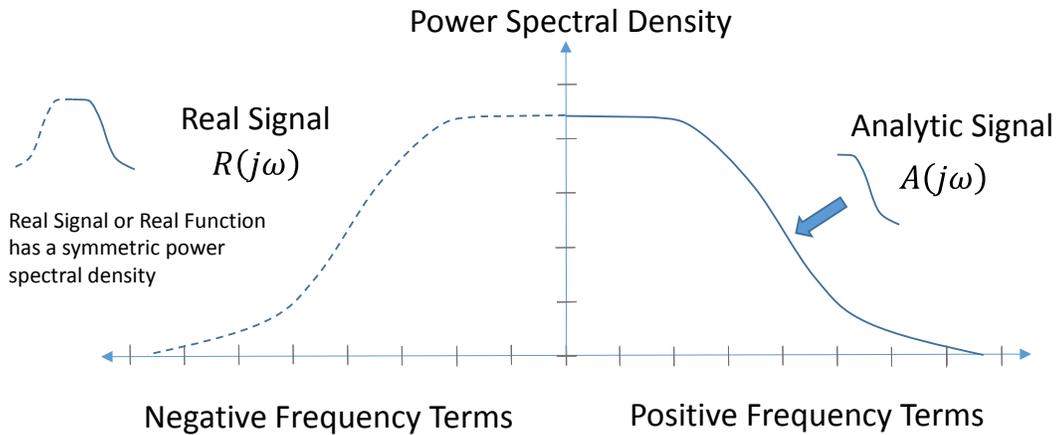
Fig. 9   Real and analytic signals

$$r(t) \Longleftrightarrow R(j\omega)$$ Fourier transform pair for a real signal.   (4)

$$R(-j\omega) = R^*(j\omega)$$ Real signals have the Fourier transform property, where * = complex conjugate.   (5)

$$A(j\omega) = \begin{cases} 2R(j\omega) & \omega > 0 \\ R(j\omega) & \omega = 0 \\ 0 & \omega < 0 \end{cases}$$ Analytic signal, $A(j\omega)$, in terms of real signal, $R(j\omega)$.

$$a(t) \Longleftrightarrow A(j\omega)$$ Analytic signal Fourier transform pair.   (6)

$$A(j\omega) = 2u(j\omega)R(j\omega)$$
$$A(j\omega) = [1 + sgn(j\omega)]R(j\omega)$$ Simplify Eq. 6.   (7)

8

$$\frac{1}{\pi t} \Longleftrightarrow -jsgn(j\omega)$$

Fourier transform pair for signum function.

$$\frac{j}{\pi t} \Longleftrightarrow sgn(j\omega)$$

(8)

$$a(t) = r(t) + F^{-1}\{sgn(j\omega)\} \otimes F^{-1}\{R(j\omega)\}$$

Simplify Eq. 8,

$$a(t) = r(t) + F^{-1}\{sgn(j\omega)\} \otimes r(t)$$

$$a(t) = r(t) + j\left[\frac{1}{\pi t} \otimes r(t)\right] \text{ (see Eq. 8)}$$

where $\otimes$ operation is convolution.

(9)

$$a(t) = r(t) + j\hat{r}(t) \text{ where } \hat{r}(t) = \frac{1}{\pi t} \otimes r(t)$$
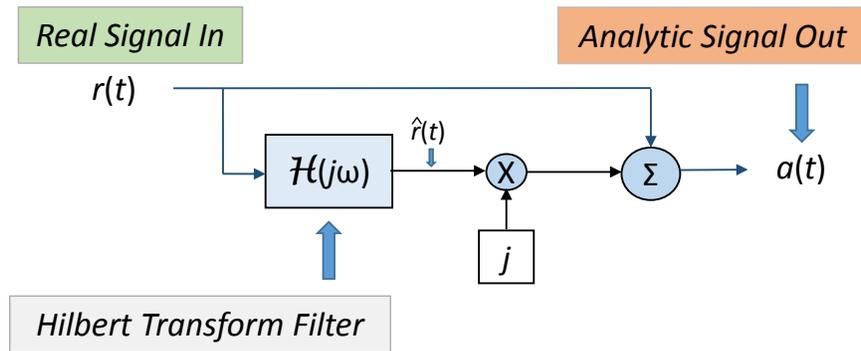
Fig. 10   Real-to-analytic signal block diagram

A block diagram showing the operations to convert a real signal to an analytic signal is found in Fig. 10. The Hilbert signal, $\hat{r}(t)$, is the Hilbert transform of $r(t)$. In digital signal processing, the Hilbert transform is typically implemented as a low-pass FIR filter (Fig. 11).
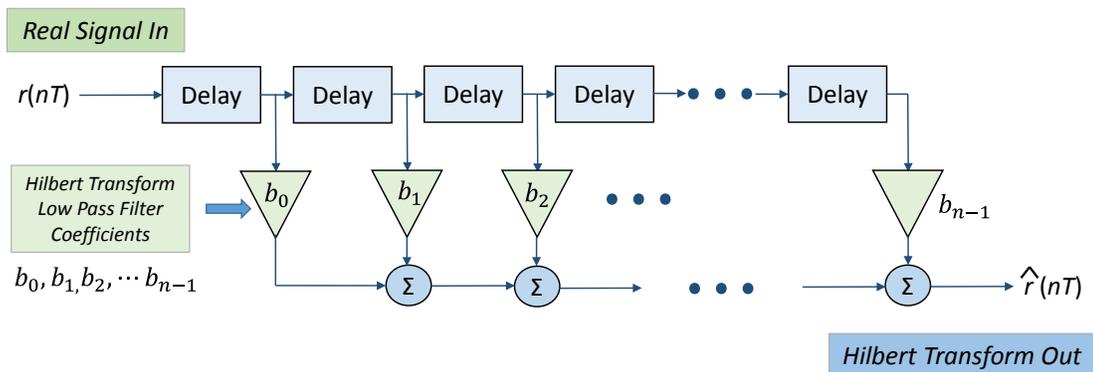
Fig. 11   Low-pass finite impulse response (FIR) Hilbert transform

A 255-tap low-pass Hilbert transform FIR filter was simulated to create the power spectral density graph in Fig. 12. A square wave and its Hilbert transform are shown in the time domain. A block diagram shows the steps required to convert a real signal to an analytic signal. The power spectral density plots compare the real square wave signal to the square wave analytic signal. The analytic signal has removed the negative frequency terms. The largest negative frequency term is 56 dB down from the input real signal.

Analytic signals are a generalization of complex exponentials. Analytic signals have the very useful frequency and phase shift properties of complex exponentials. The simple frequency translation and phase shift properties of analytic signals make them very useful for digital signal processing.

11
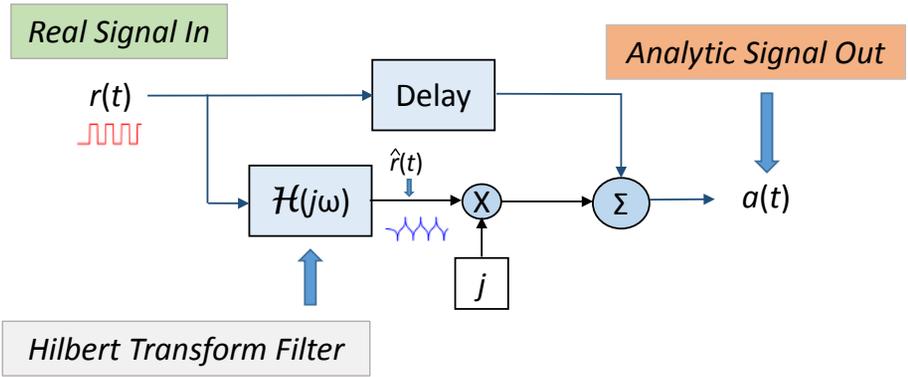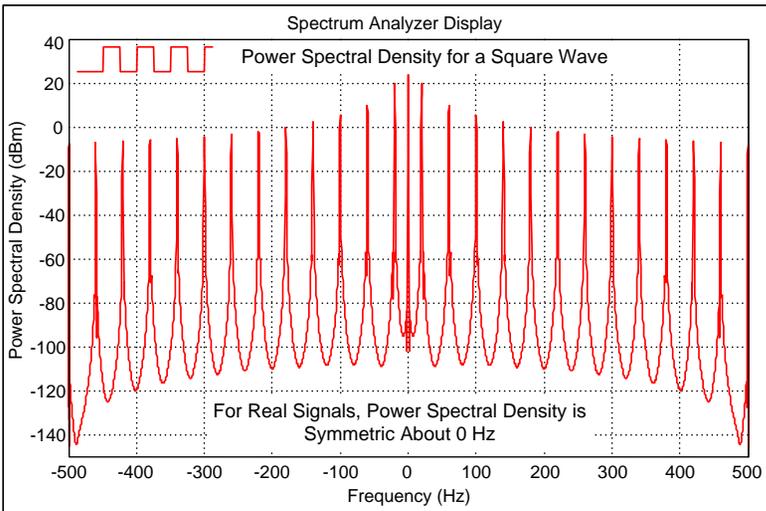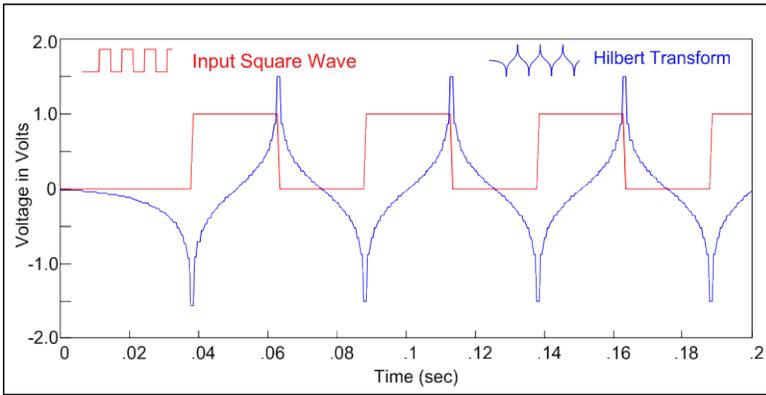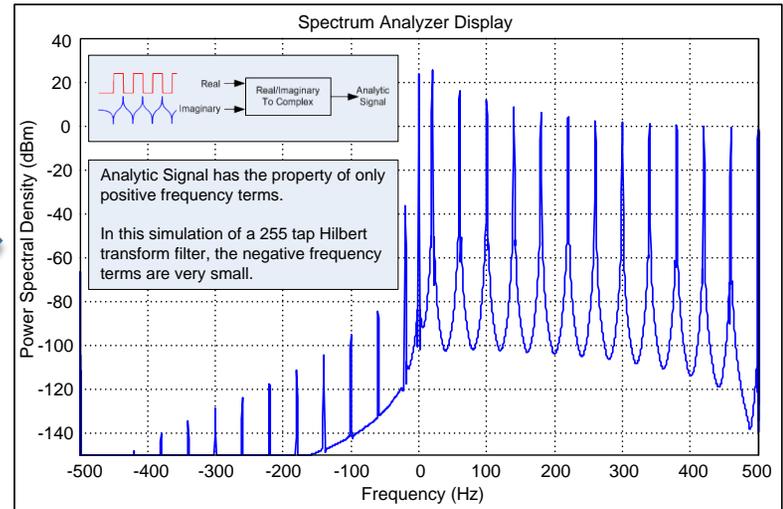
Fig. 12   Hilbert transform and analytic signals

As an example, a high-frequency (1–30 MHz) software-defined radio (SDR) is illustrated in Fig. 13. We have shown a double conversion analog front end. With a 120 Msample/s, 14-bit analog-to-digital converter (ADC), we could connect the ADC directly to the antenna. Analog front-end radios still have a higher dynamic range than completely digital SDRs. The SDR in Fig. 13 provides a 14-bit ADC running at 2 times oversampling. The oversampling provides about 3 more decibels of dynamic range. The sampling frequency for the digital I/Q output is 20 Msamples/s with about 87 dB of digital dynamic range. Analog automatic gain control (not shown) could provide more useable dynamic range.
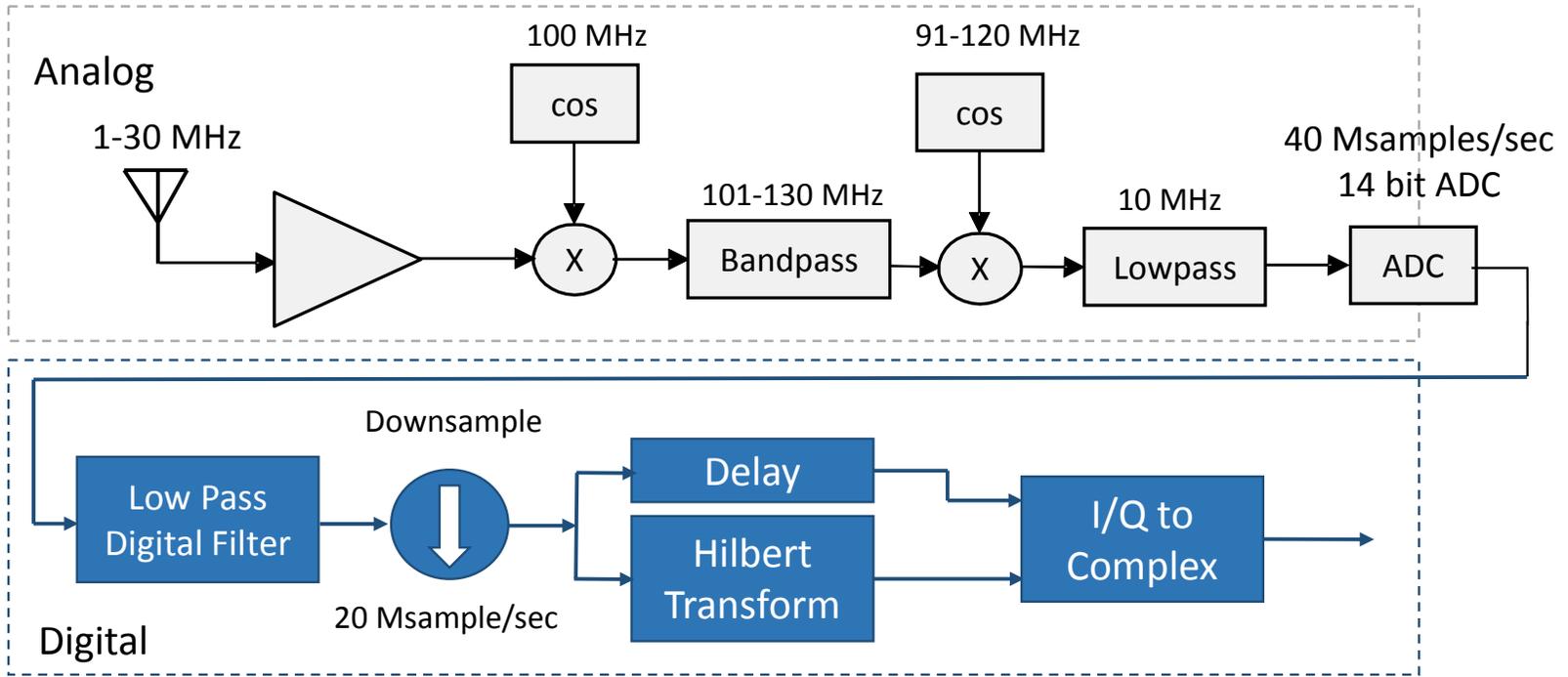
Fig. 13   Example high-frequency double radio frequency conversion, digital software-defined radio

13

3.   Digital Signal Processing in a Software-Defined Radio

Figure 14 illustrates an example of an SDR architecture for a high-frequency receiver, with a double conversion analog front end. ADCs have limited dynamic range. As ADCs have improved, the analog-to-digital conversion step has moved closer to the antenna. Analog front ends currently have better dynamic range and overload protection. Figure 14 illustrates a 40 Msample/s, 14-bit ADC. For the 10-MHz intermediate frequency (IF); this is 2 times oversampling.
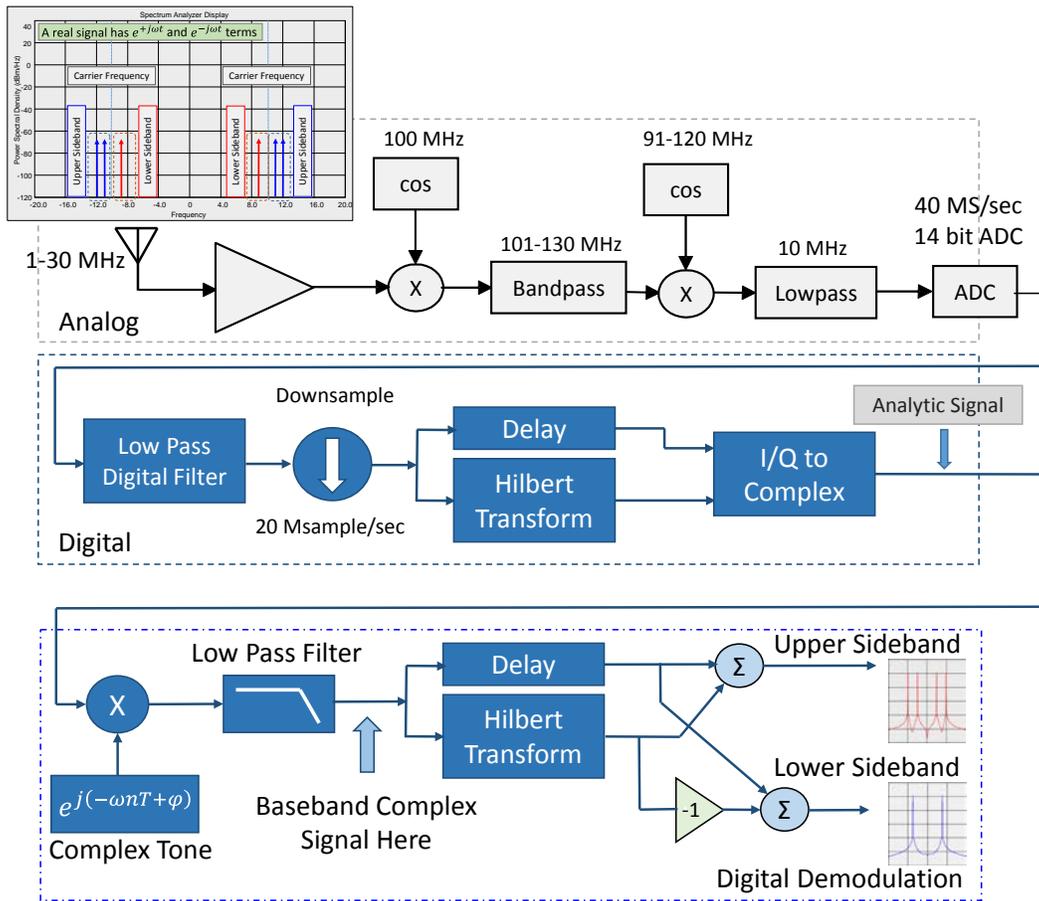
Fig. 14   Example upper and lower sideband software-defined radio

Figure 15 shows the power spectral density for the received signal. We use Dirac delta functions to show power concentrated at single frequencies. The upper sideband consists of 2 tones. The lower sideband has a single tone. The digital block in Fig. 14 converts the real signal to an analytic signal. We use a complex tone (complex exponential function) to convert the center frequency to 0 Hz (DC).
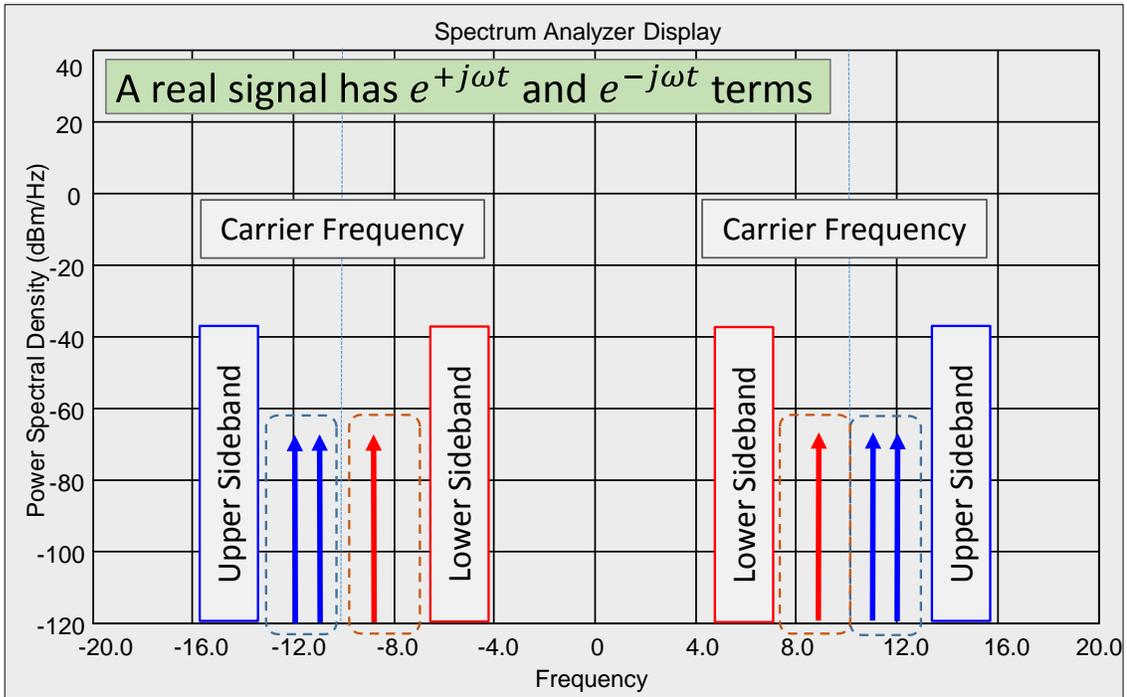
Fig. 15   Received power spectral density

A second Hilbert transform in the digital demodulation block is used to separate the upper and lower sidebands from the complex baseband signal.

Figure 14 illustrates the usefulness of the Hilbert transform to 1) convert a real signal to an analytic signal and 2) demodulate single sideband. Figure 16 shows the real power spectral density for the upper sideband, and Fig. 17 shows the real power spectral density for the lower sideband. Since the power spectral densities are real signals, upper and lower sideband signals can drive a speaker.

The analog hardware in Fig. 14 is fixed. It can be upgraded with new analog hardware. The digital blocks in the example SDR architecture are software. Signal processing and filtering algorithms can be upgraded with new software.
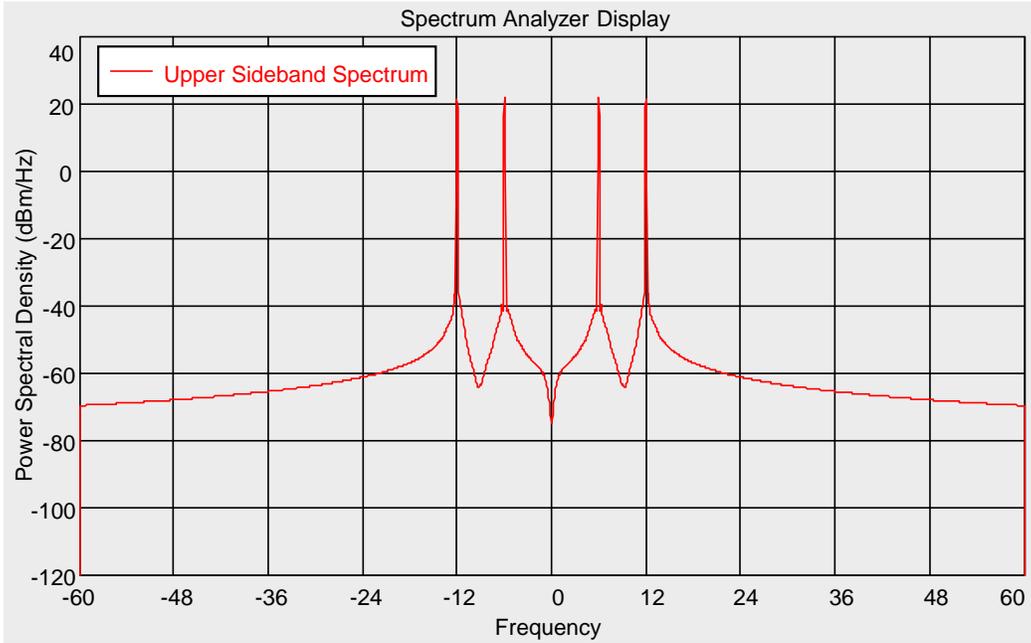
Fig. 16   Upper sideband spectrum
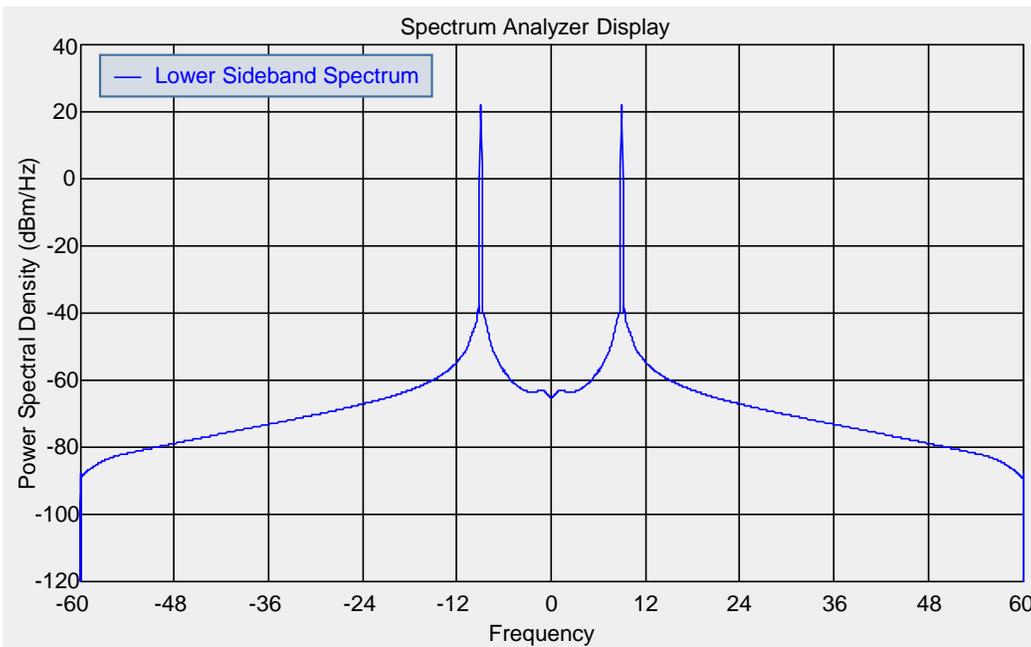
Fig. 17   Lower sideband spectrum

16

Figure 18 compares frequency shift keying (FSK) and Feher FSK.[1–6] Feher modulation replaces the sharp pulse transitions in frequency shift keying with half-cycle raised cosine waveforms. As illustrated in the simulation in Fig. 18 (see the Comm page of the VisSim website[7] for more information about the simulation tool), Feher modulation uses half-cycle raised cosine waveforms to create smooth transitions between symbols. With an SDR architecture, we could easily upgrade FSK to Feher FSK with a new software program.
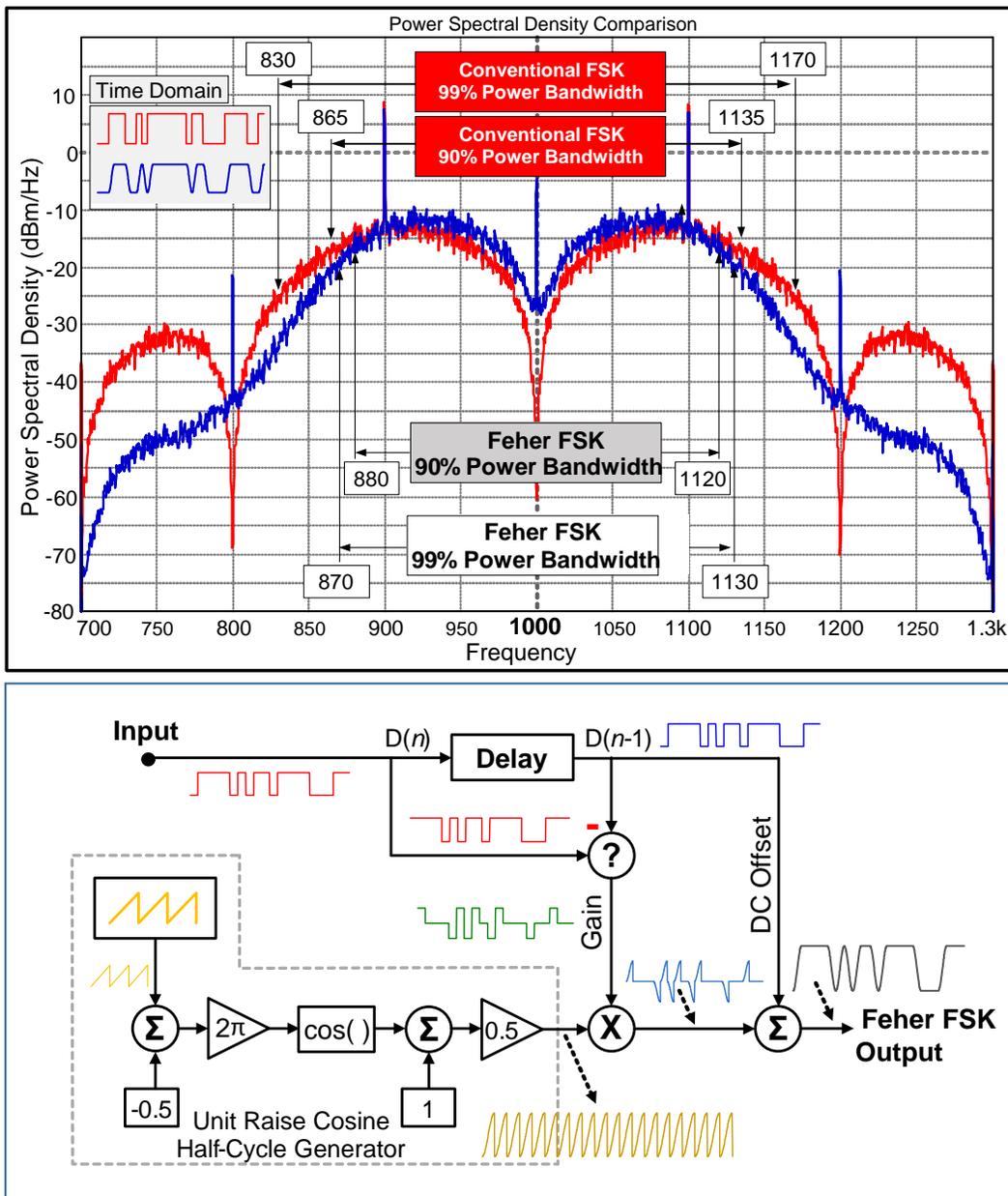
Fig. 18   Frequency shift keying and Feher frequency shift keying

An example of an SDR transmitter block diagram is shown in Fig. 19. Here, we illustrate a software upgrade from standard quadrature amplitude modulation (QAM) to Feher QAM[1–6]. Feher QAM provides improved radio performance at the expense of some additional signal processing. As illustrated, Feher modulation smooths out the sharp symbol transitions, reducing the bandwidth required. Feher modulation also has much-improved frequency sidelobes as illustrated in Fig. 20.
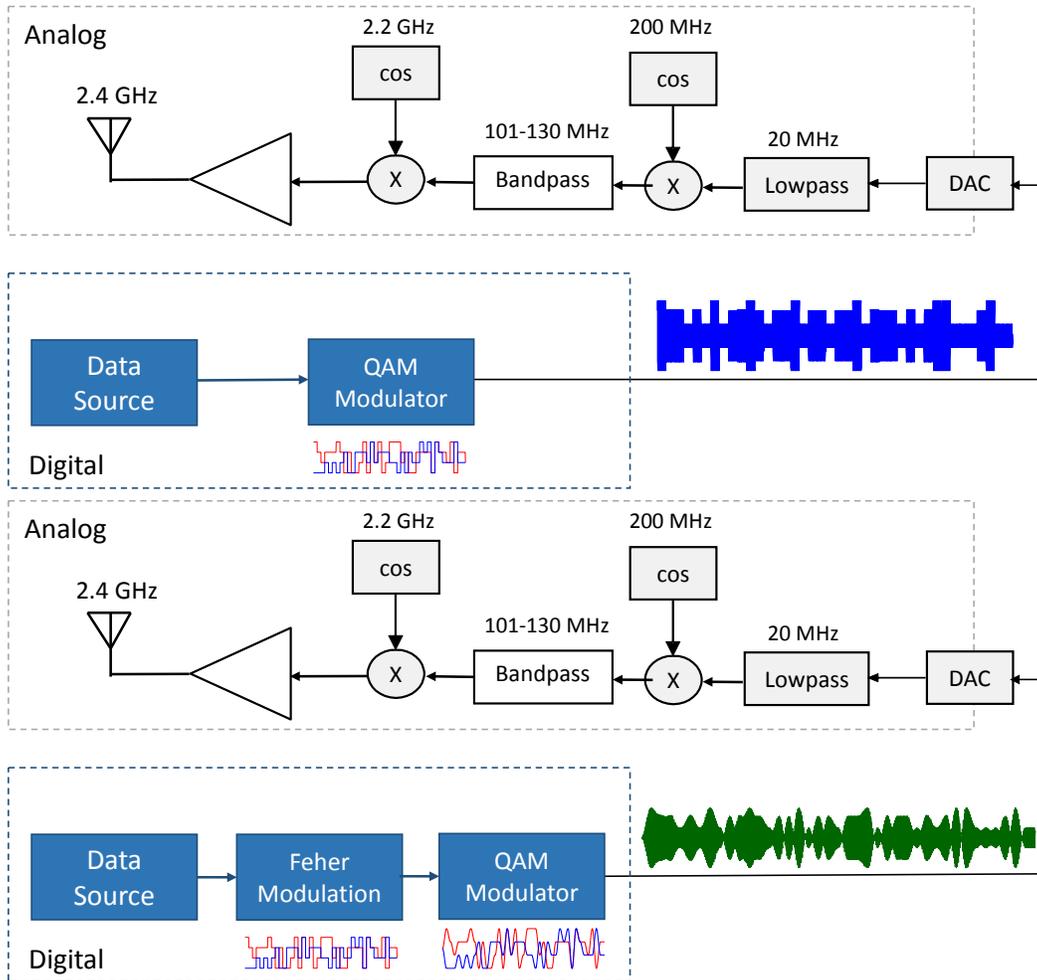
Fig. 19   Quadrature amplitude modulation software-defined radio example
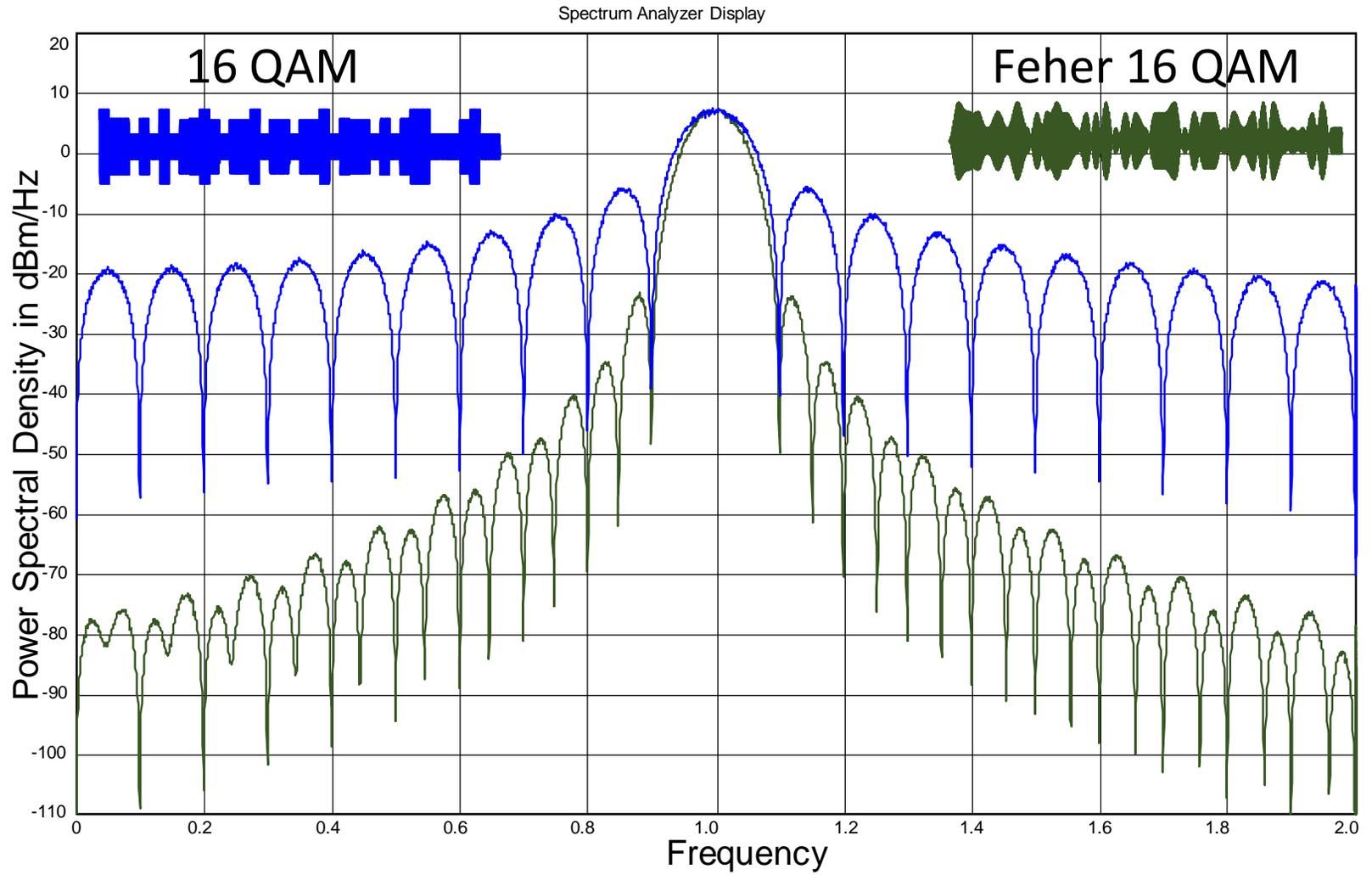
Fig. 20   Power spectral density for 16 QAM and Feher 16 QAM

4.   Conclusion

We present an introduction to digital signal processing for an SDR. We illustrate the advantages of analytic signals for frequency translation and phase shift. Two SDR algorithm (software) upgrade examples are provided.

5.   References

1.   Feher K, inventor. Filter. United States patent US 4,339,724. 1982 Jul 13.

2.   Simon P, Yan T. Performance evaluation and interpretation of unfiltered feher-patented quadrature-phase-shift keying (FQPSK). Greenbelt (MD): National Aeronautics and Space Administration; 1999 May 15. NASA TMO Progress Report 42–137 [accessed 2016 Oct 14]. http://ipnpr.jpl.nasa.gov/progress_report/42-137/137C.pdf.

3.   Simon M, Divsalar D. Further results on a reduced-complexity, highly power/bandwidth-efficient coded feher-patented quadrature-phase-shift-keying system with iterative decoding. Greenbelt (MD): National Aeronautics and Space Administration; 2001 Aug 15. NASA IPN Progress Report 42–146 [accessed 2016 Oct 14]. http://tmo.jpl.nasa.gov/progress_report/42-146/146I.pdf.

4.   Wang S. Bandwidth efficient aeronautical telemetry modem and transceiver research. Davis (CA): University of California, Davis; 1998 Sep. Final Report Grant No.: AFOSR F49620-98-1-0097 [accessed 2016 Oct 14]. www.dtic.mil/get-tr-doc/pdf?AD=ADA386772.

5.   Jungwirth P. Smoothed symbol transition modulation. AlaSim International Conference and Exposition. 2014 May 6–7; Huntsville, AL.

6.   Jungwirth P. Smoothed symbol transition modulation digital signal processing algorithm. TAPR Conference; 2014 Sep 5–7; Austin, TX. p. 32–51 [accessed 2016 Oct 14]. https://www.tapr.org/pdf/DCC2014-SmoothedSymbolTransitionModulation-Patrick-Jungwirth.pdf.

7.   Visual Solutions. VisSim/Comm; 2016 [accessed 2016 Nov 7]. http://www.vissim.com/products/vissim/comm.html.

INTENTIONALLY LEFT BLANK.

Appendix. Review of Complex Numbers

In this Appendix, we present a review of complex numbers. We start with a simple number line for a bottom-up approach to explain the properties of complex numbers and then illustrate that complex numbers are built from real numbers. In digital signal processing, the multiplication property of complex numbers (analytic functions) provides for simple frequency translation and phase shift.

We will take a geometric approach using distance from a number line and build up to the complex plane. The bottom-up approach will review $(-1)(-1) = +1$ to help bridge the gap to complex numbers, where $i = \sqrt{-1}$, and $i^0 = +1$, $i^1 = i$, $i^2 = -1$, $i^3 = -i$, and $i^4 = +1$. The periodic behavior of i^n is a more general result than $+1 = (-1)^2$. Mathematicians use $i = \sqrt{-1}$ for the imaginary number. Since $i(t)$ is the traditional variable for electrical current, electrical engineers use $j = \sqrt{-1}$.

A.1 Number Lines and Planes

The number line in Fig. A-1 shows positive numbers 0, 1, 2, 3, 4, •••. A number line showing directions, East and West, is used to bridge the gap to negative numbers. In measuring distance on a number line, we show that $(-1)(-1) = +1$, negative 1 times negative 1 equals a positive 1. Intuitively, the equation $+1 = (-1)(-1)$ appears incorrect. With a 2-D plane, also called the Cartesian plane, we provide a simple geometric illustration to show that $+1 = (-1)(-1)$ is a special case from the complex plane.

What is the distance from 2 to 9 on the number line?

Fig. A-1   Number line

Distance is the measurement length from point a on the number line to point b. Distance is a positive number and does not indicate direction. Distance, $d = |b - a|$, is found in Eq. A-1, where the $|\quad|$ operation is the absolute value function. For example, $|5| = 5$ and $|-5| = 5$. The distance from point a on the number line to point b is the same as the distance from b on the number line to point a.

$$d = |b - a| \quad \text{Distance from point } a \text{ to point } b \quad \text{(A-1)}$$

The distance from 2 to 9, as shown in Fig. A-1, is $d = |b - a| = |9 - 2| = 7$.

The distance from 7 to 3 is $d = |3 - 7| = |3 - 7| = 4$.

The directional distance is defined as $\Delta = b - a$ in Eq. A-2. For directional distance, the sign of Δ tells us if we are moving on the number line to the right or to the left.

For example, the directional distance from 8 to 3 is $\Delta = 3 - 8 = -5$. The distance -5 tells us we are moving 5 steps to the left or 5 steps to the West. The directional distance from 4 to 9 is $\Delta = 9 - 4 = 5$. The distance 5 tells us we are moving 5 steps to the right or East.

$$\Delta = b - a \qquad \text{Directional Distance} \qquad \text{(A-2)}$$

In Fig. A-2, we have borrowed the compass points East and West for left and right directions. How do we compute the distance from point a to b in Fig. A-2? Point a is located at 5 East and point b is located at 4 West. From Eq. A-1, we have distance $d = |b - a|$. 5 East is 5 steps from 0, and 4 West is 4 steps from 0. The total distance is then $5 + 4 = 9$ in Eq. A-3. The point b at 4 West is -4 in the East direction, so we may rewrite Eq. A-3 as Eq. A-4. From a distance and geometry point of view, we have shown that $-(-4)$, minus -4, is the same thing as $+4$.
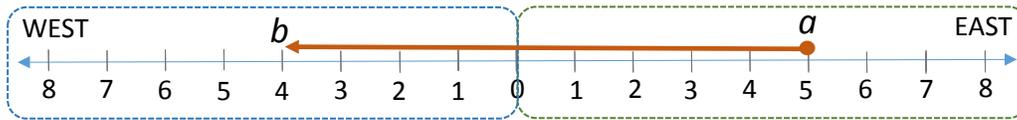
Fig. A-2 East–West number line

$$d = |b - a| = |5\ East - 4\ West| = 9. \qquad \text{(A-3)}$$

$$d = |b - a| = |5\ East - (-4)\ East| = 9. \qquad \text{(A-4)}$$

For directional distance a negative is used to indicate direction to the *left* and positive direction to the *right*. Figure A-2 used East and West for directions. In Fig. A-3, we use negative numbers for the West direction and positive numbers for the East direction. The distance between points a and b in Fig. A-3 is found in Eq. A-5. We have $|-3 - 2| = |-5| = 5$. In Fig. A-3, we can clearly see the distance from $a = +2$ to $b = -3$ is 5 units.
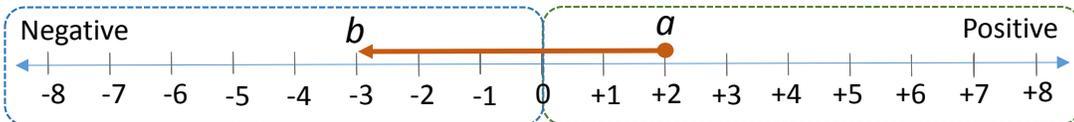
Fig. A-3 Positive and negative number line (Example 1)

$$d = |b - a| = |-3 - 2| = 5. \qquad \text{(A-5)}$$

What is the difference between minus 2 and negative 2? Negative 2 is located at 2 steps (to the left) from 0 on the number line. The math operation minus 2 means to move 2 steps back on the number line. For minus -2, we move 2 steps backwards from -2, which is the same as moving 2 steps forward. From a number line point

of view, the operation minus –2 can be simplified to –(–2) = (–1)(–1)2 = 2 (negative 1 times a negative 1 = + 1).

Here, we continue the discussion of minus –*n* (where –*n* is a negative number). We will use distance, which is defined as a positive number, to explain what minus –*n* means. In Fig. A-4, we have point *a* at –5, which is 5 steps to the left of zero. Point *b* is 3 steps to the right of 0. The total distance is 5 + 3 = 8. Figure A-4 and Eq. A-5 show from a geometry point of view that minus –5 is the same thing as +5.

From the positive and negative number line in Fig. A-4, we have shown that –5 is 5 steps from 0 and minus –5 is equivalent to moving 5 steps to the right. Starting at *a* = –5, we move 5 steps to 0 and then move 3 more steps to *b* = +3. The total distance is 8 steps. The example in Fig. A-4 illustrates minus -*n* (-*n* is a negative number) is the same as +*n*.
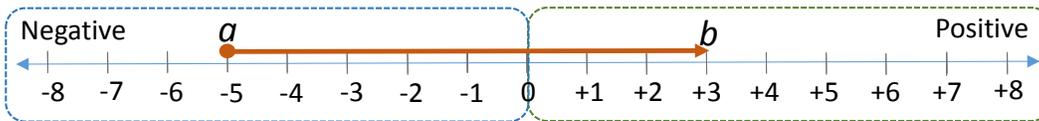
Fig. A-4   Positive and negative number line (Example 2)

$$d = |b - a| = |+3 - (-5)| = 8. \tag{A-5}$$

The East-West or positive and negative numbers for a number line are a notation. We need to know the "rules" for addition and subtraction to compute distance in Eq. A-1. We will extend the number line in Fig. A-4 to 2 dimensions to create the Cartesian plane. We can then use positive and negative numbers for the *x*-axis and *y*-axis or we can use the cardinal compass points. The 2-D graph allows us to bridge from real to complex numbers.

In Figs. A-5 and A-6, we show that a number line can be extended into 2 dimensions. The point *P* can be represented in Cartesian space as $P = (x, y) = (-1.5, -0.75)$ or in terms of compass points $P = (x, y) = (1.5W, 0.75S)$. Polar coordinates are another way of representing points on a 2-D graph. Eq. A-6 shows how to convert rectangular coordinates in terms of (x, y) into polar coordinates (r, θ). As we will show in the next section, the polar coordinates for the Cartesian plane in Fig. A-7 and the complex number plane in Fig. A-8 are equivalent. What makes complex numbers useful for digital signal processing are the frequency translation and phase shift properties of complex exponential functions.

$$(r, \theta) = \left(\sqrt{x^2 + y^2}, tan^{-1}\left(\tfrac{y}{x}\right) \right). \tag{A-6}$$

$y-axis$

By adding a second number line in the y-direction, we extend the number line in the x-direction

$x-axis$

-2   -1   1   2

P

$(x, y) = (-1.5, -0.75)$

Fig. A-5   Cartesian graph

North

Compass points: N, S, E, and W are another notation for +/- y axis, and +/- on the x axis

West   East

2   1   1   2

P

$(x, y) = (1.5W, 0.75S)$
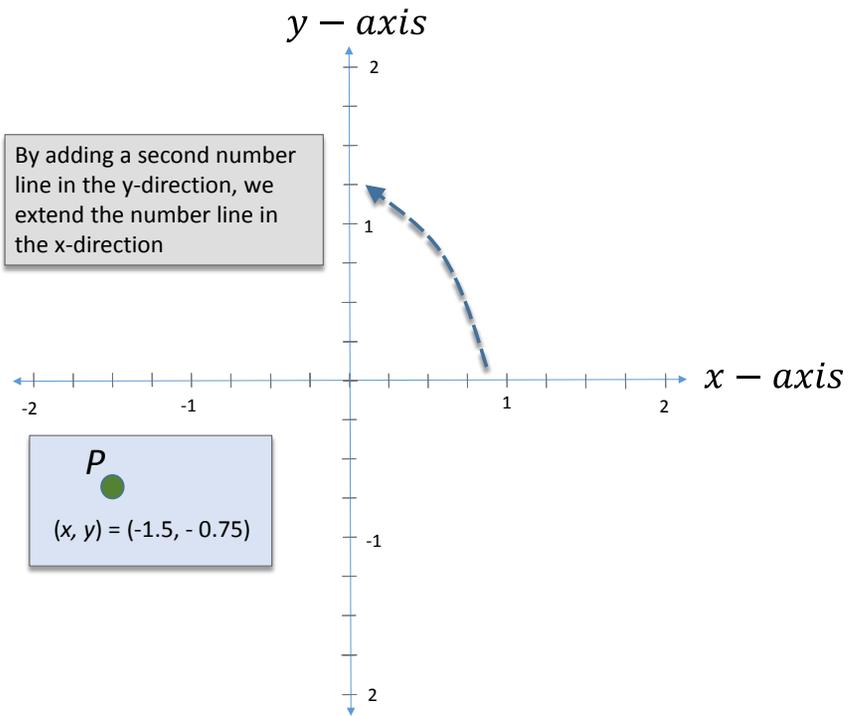
South
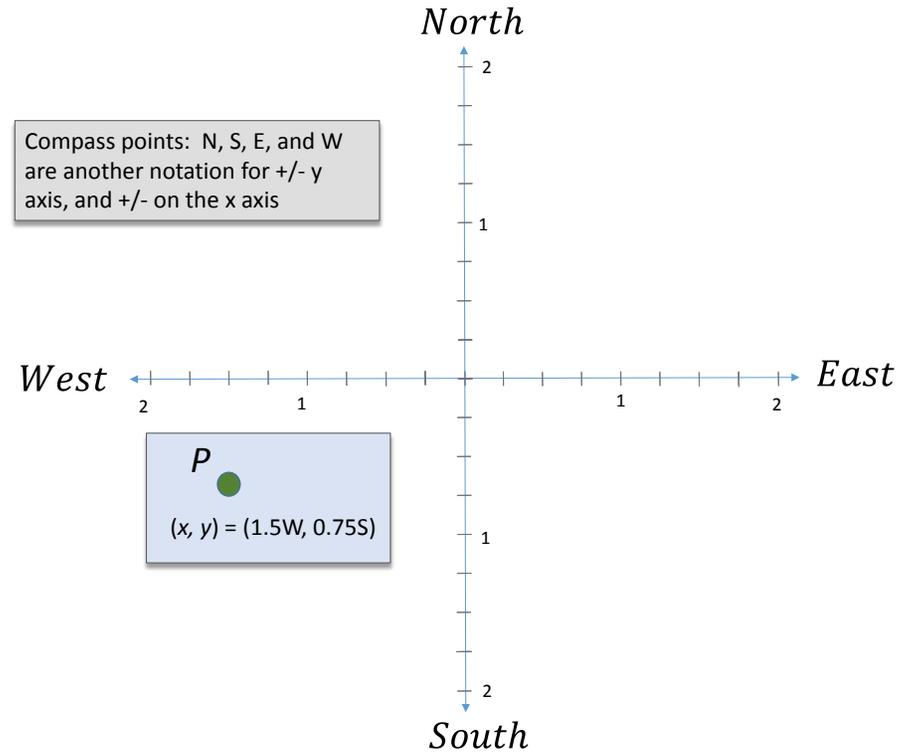
Fig. A-6   Compass point graph

2

Unit Circle

1

(x, y)
(r, θ)

radius
r

Angle
θ

-2   -1   1   2

-1

$(x, y) = (r cos θ, r sin θ)$ where

$(r, θ) = \left(\sqrt{x^2 + y^2}, tan^{-1}\left(\frac{y}{x}\right) \right)$

2

Fig. A-7   Cartesian graph

+2j

Unit Circle

+j

x + jy

(r, θ)

radius
r

Angle
θ

-2   -1   1   2

-j

radius is $r = \sqrt{x^2 + y^2}$
angle is $θ = tan^{-1}\left(\frac{y}{x}\right)$

-2j

Fig. A-8   Complex number graph

A.2 Square Root and Complex Numbers

In Section A.1, number lines and planes introduced the connection between 2-D Cartesian space and complex planes. We found that the polar coordinate form is the same for the Cartesian space and the complex plane. In this section, we will start with the square root function and define imaginary numbers. Polar coordinates are then used to derive the complex exponential function. The complex exponential function's frequency translation and phase shift properties are very useful for digital signal processing.

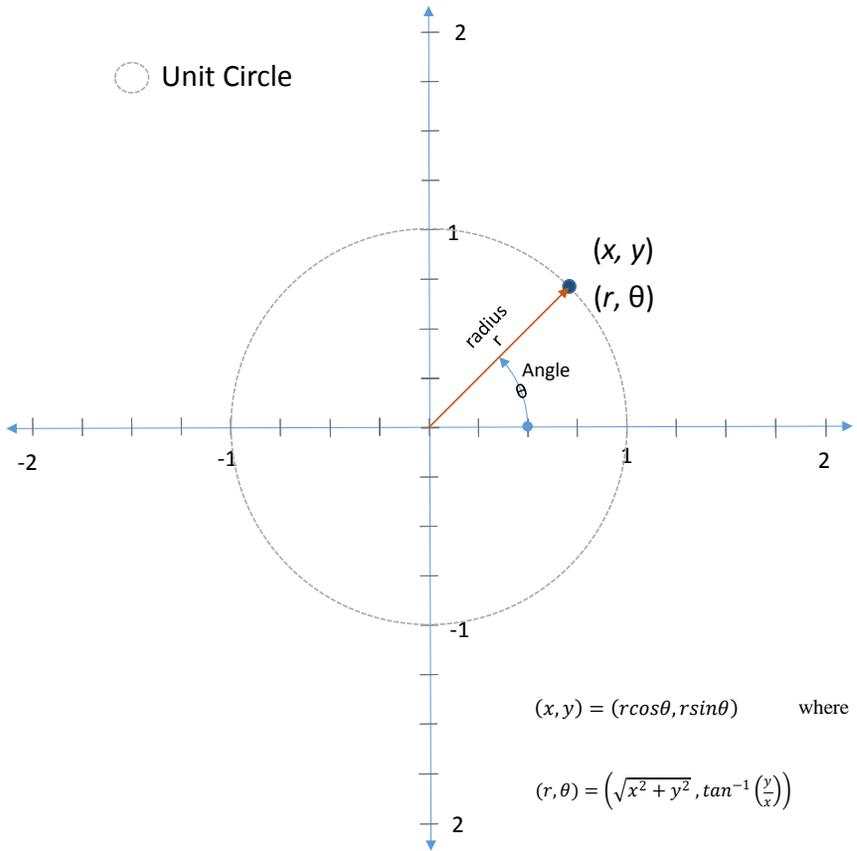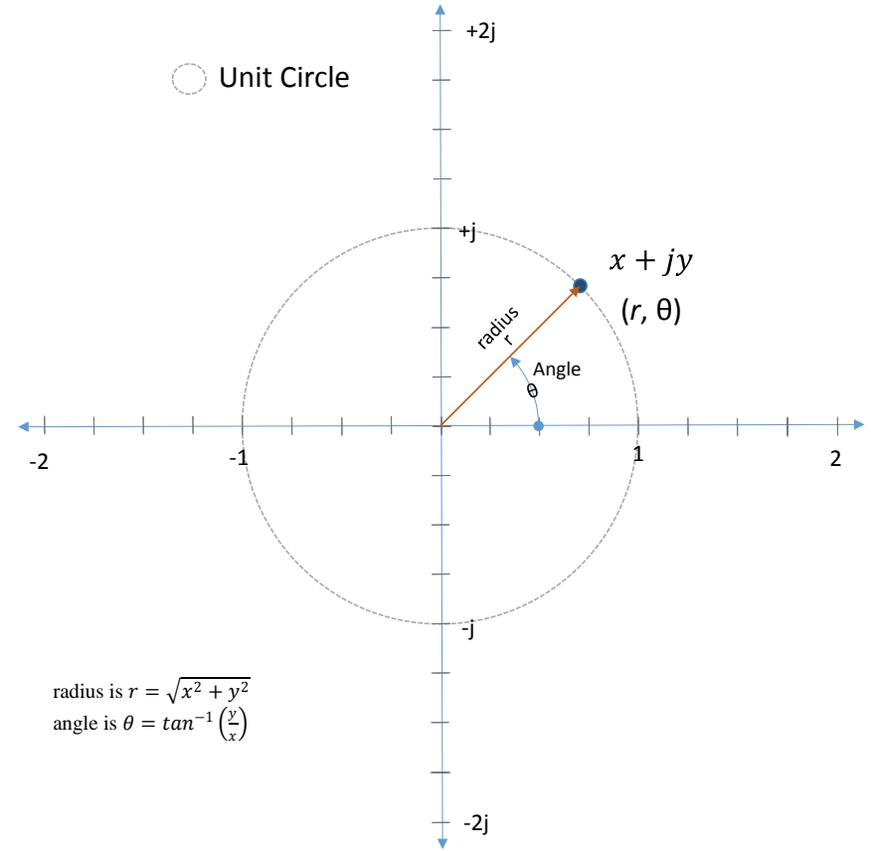The square root function is graphed in Fig. A-9. For positive numbers, the square root function is straightforward. What number squared equals x? For example, $1^2 = 1$, $2^2 = 4$, and $3^2 = 9$. What number squared equals negative 1? We observe for the square root function $y^2 = x$. We will define $j^2 = -1$. This fits the pattern shown in Fig. A-8. With $j^2 = -1$, the square root gives $j = \sqrt{-1}$. In Figs. A-5 and A-7, we have graphed real numbers. The real numbers are ••• –3, –2, –1, 0, +1, +2, +3, •••. The number line defined in terms of $j = \sqrt{-1}$ does not appear to have a connection to real numbers. The numbers ••• –3j, –2j, –1j, 0, +1j, +2j, +3j, ••• are called imaginary numbers. If we add 2 real numbers, $5 + 7 = 12$, the result is a real number. If we add a real number to an imaginary number, $3 + 2j = 3 + 2j$, we cannot combine the 3 and the 2 into a single number. The numbers 3 and 2j are called linearly independent. Linearly independent means we cannot reduce $3 + 2j$ into a simpler number. The Cartesian graph in Fig. A-5 also demonstrates linear independence. We need an x position and a y position to graph a point on the graph. We cannot take the point $(x, y) = (1, 2)$ and plot 3 on the graph.
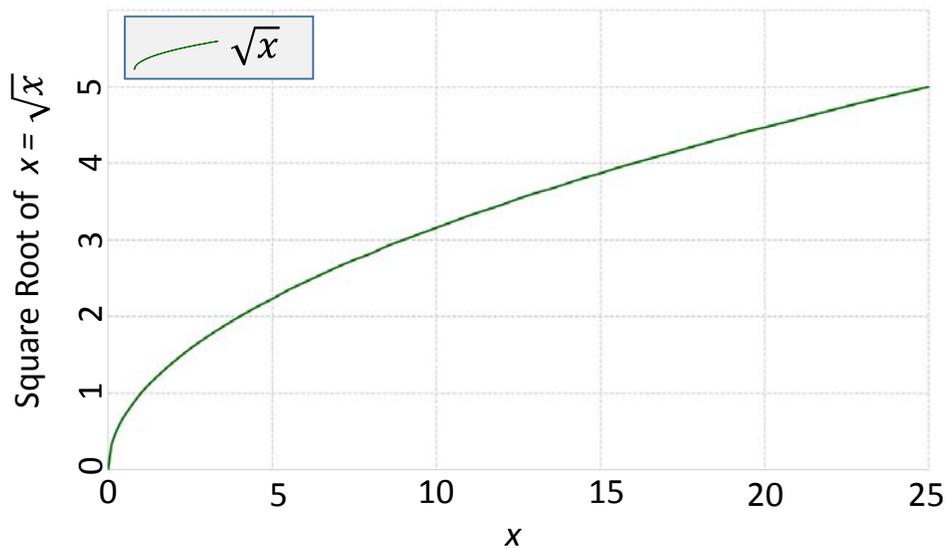

Fig. A-9 Square root of x

The number $3 + 2j$ is called a complex number. A complex number $(a + jb)$ contains a real part, a, and an imaginary part, jb. The numbers a and b are both real numbers. The imaginary constant j separates the real and imaginary parts. In Fig. A-8, we use the linear independence property to graph the real numbers on the x-axis and the imaginary numbers on the y-axis. Polar coordinates in Eq. A-7 are multivalued. More on the properties of complex numbers in the following sections.

$$(r, \theta) = (r, \ (\theta + 2k\pi)) \quad \text{where } k \text{ is an integer.} \tag{A-7}$$

Figures A-7 and A-8 show that polar coordinates connect the Cartesian plane to complex numbers in the complex plane. The (x, y) values represent a coordinate in the Cartesian plane as illustrated in Fig. A-7. The complex number $x + jy$ represents a point in the complex plane as shown in Fig. A-8. The values for x and y in the Cartesian coordinate notation (x, y) in Eq. A-8 and complex number notation $x + jy$ in Eq. A-9 are the same. The polar equation form in Eq. A-10 shows how to convert from Cartesian and complex numbers to polar form. Next, we show the connection between the complex exponential in Eq. A-11 and polar equation form in Eq. A-10. In digital signal processing, the properties of the complex exponential form provide for simple frequency translation and phase shift.

Cartesian Plane		
$(x, y) = x\vec{x} + y\vec{y}$ where	$\vec{x}$ is the unit vector for the x-coordinate $\vec{y}$ is the unit vector for the y-coordinate	(A-8)

Complex Plane		
$x + jy$ where	x is the real part of the complex number jy is imaginary part of the complex number	(A-9)

Polar Coordinates		
$(x, y) = (r\cos\theta, r\sin\theta)$ where	radius is $r = \sqrt{x^2 + y^2}$ angle is $\theta = \tan^{-1}\left(\frac{y}{x}\right)$	(A-10)
$x + jy = r(\cos\theta + j\sin\theta)$	complex form	(A-11)

To show the connection between polar coordinates and the complex exponential, we start with Fig. A-7, $r = 1$ (the unit circle). In Eq. A-11, we let the radius $r = 1$, as shown in Eq. A-12. Equations A-13 through A-15 show the infinite series for $sin\theta$, $cos\theta$, and e^x, respectively. In Eq. A-16, we expand e^x with $x = j\theta$. We find the infinite series in Eq. A-17 for sine and cosine, as shown in Eq. A-18. In Eq. A-19, we present the Euler form for a complex exponential.

$$x + jy = (cos\theta + jsin\theta) . \tag{A-12}$$

$$sin\theta = \theta - \frac{\theta^3}{3!} + \frac{\theta^5}{5!} - \frac{\theta^7}{7!} + \cdots \tag{A-13}$$

$$cos\theta = 1 - \frac{\theta^2}{2!} + \frac{\theta^4}{4!} - \frac{\theta^6}{6!} + \cdots \tag{A-14}$$

$$e^x = 1 + x + \frac{x^2}{2!} + \frac{x^3}{3!} + \frac{x^4}{4!} + \cdots \tag{A-15}$$

$$e^x = 1 + x + \frac{x^2}{2!} + \frac{x^3}{3!} + \frac{x^4}{4!} + \cdots \text{ with } x = j\theta. \tag{A-16}$$

$$e^{j\theta} = 1 + j\theta + \frac{(j\theta)^2}{2!} + \frac{(j\theta)^3}{3!} + \frac{(j\theta)^4}{4!} + \frac{(j\theta)^5}{5!} + \frac{(j\theta)^6}{6!} \cdots =$$
$$\left(1 + \frac{(j\theta)^2}{2!} + \frac{(j\theta)^4}{4!} + \frac{(j\theta)^6}{6!} + \cdots\right) + \left(j\theta + \frac{(j\theta)^3}{3!} + \frac{(j\theta)^5}{5!} + \cdots\right) \tag{A.17}$$
$$\left(1 - \frac{\theta^2}{2!} + \frac{\theta^4}{4!} - \frac{\theta^6}{6!} + \cdots\right) + j\left(\theta - \frac{\theta^3}{3!} + \frac{\theta^5}{5!} - \frac{\theta^7}{7!} \cdots\right)$$

where $j = \sqrt{-1}$, and $i^0 = +1, j^1 = j, j^2 = -1, j^3 = -i$, and

$j^4 = +1$ and $j^5 = jj^4 = j$

$$(cos\theta + jsin\theta) = 1 - \frac{\theta^2}{2!} + \frac{\theta^4}{4!} - \frac{\theta^6}{6!} + \cdots j\left[\theta - \frac{\theta^3}{3!} + \frac{\theta^5}{5!} - \frac{\theta^7}{7!} + \cdots\right]. \tag{A-18}$$

$$e^{j\theta} = (cos\theta + jsin\theta). \tag{A-19}$$

In complex exponentials, simple multiplication is used for frequency translation as illustrated in Eq. A-20. Frequency translation only results in a single frequency term. For real sine and cosine functions, frequency translation results in sum and difference terms (2 terms). Sine and cosine functions require an additional high-pass or low-pass filter to separate the sum or difference term. Phase shift in complex exponentials is also a simple multiplication in Eq. A-21. Phase shift in real sines and cosines is too difficult to work with.

$$f(t) = e^{j\left(2\pi f_1\ t\right)}, \text{ and } g(t) = e^{j\left(+2\pi f_2\ t\right)}$$

$$f(t)g(t) = e^{j\left(2\pi f_1\ t\right)} = e^{j\left(-2\pi f_2\ t\right)} = e^{j\left(2\pi\left(f_1\ +f_2\ \right)t\right)} \text{ Frequency translation } f_1\ + f_2 \quad \text{(A-20)}$$

$$f(t) = e^{j\left(2\pi f_1\ t\right)}, \text{ and } g(t) = e^{j\varphi}$$

$$f(t)g(t) = e^{j\left(2\pi f_1\ t\right)}e^{j\varphi} = e^{j\left(2\pi f_1\ t+\varphi\right)} \qquad \text{Phase shift by } \varphi \text{ radians} \qquad \text{(A-21)}$$

In steady-state AC circuits, we work with rotating vectors called *phasors*. Equation A-22 shows the general form for a phasor. The Laplace transform variable *s* is closely related to a rotating vector.

$$f(t) = Ae^{j\left(2\pi f_1\ t+\varphi\right)} \text{ where A is a complex constant, } A = Re^{j\theta} \qquad \text{(A-22)}$$

From Fig. A-10 and Eq. A-19, we can calculate the $(j)^n$ in Eq. A-23. We show in Fig. A-10 the sequence j^n and illustrate the more general case of $(-1)(-1) = 1$. The magnitude stays a constant 1. The phase rotates $n\frac{\pi}{2}$ radians $(0, \frac{\pi}{2}, \pi, \frac{3\pi}{2}, 2\pi \cdots)$. Each multiplication of $e^{j\frac{\pi}{2}}$ adds $\frac{\pi}{2}$ radians. For complex exponential multiplication, the magnitudes are multiplied and the phase angles added.

$$j = \left(cos\frac{\pi}{2} + jsin\frac{\pi}{2}\right) = e^{j\frac{\pi}{2}}$$

$$j^n = \left(e^{j\frac{\pi}{2}}\right)^n = e^{jn\frac{\pi}{2}} = 1, e^{j\frac{\pi}{2}}, e^{j\pi}, e^{j\frac{3}{2}\pi}, e^{j2\pi} \cdots = 1,\ j,\ -1,\ -j,\ 1, \cdots$$
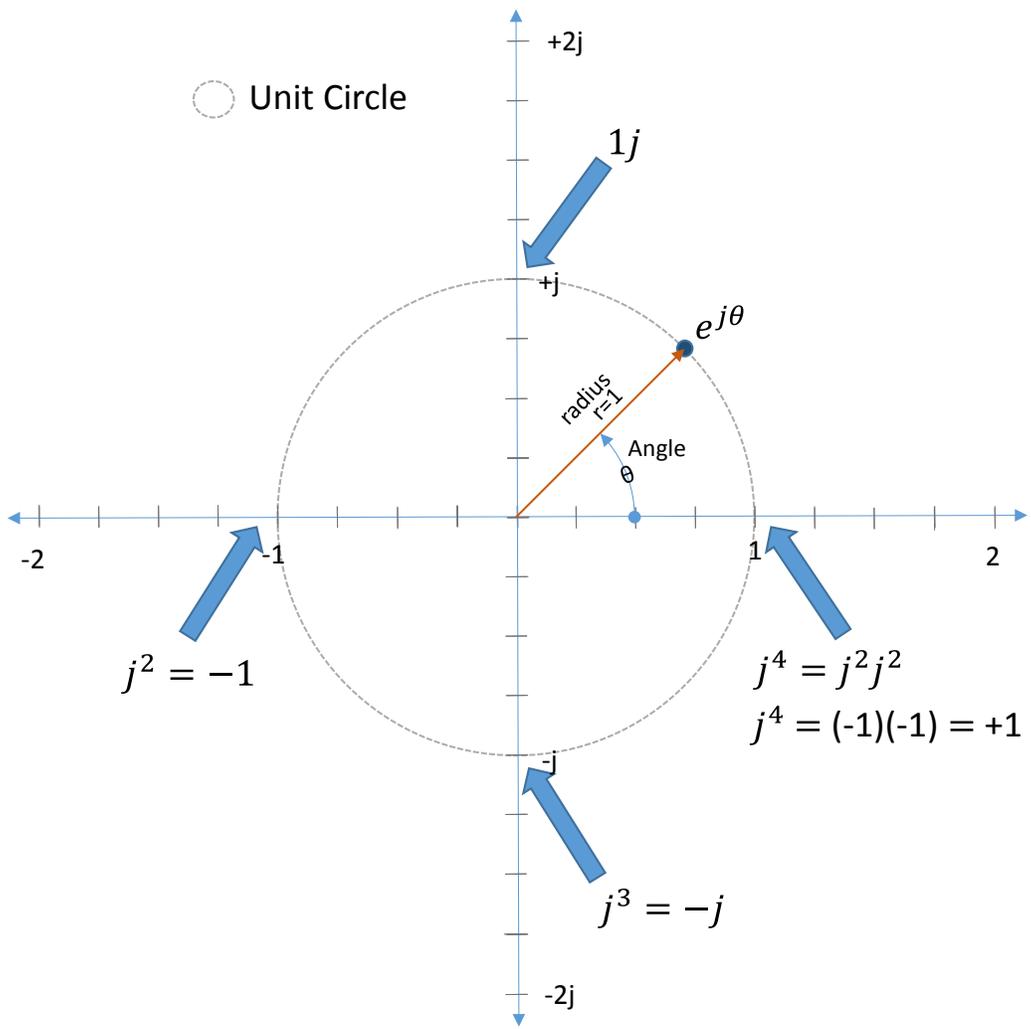
$$\text{(A-23)}$$

Fig. A-10   Complex multiplication

INTENTIONALLY LEFT BLANK.

Bibliography

Antoniou A. Digital filters: analysis, design, and applications. 2nd ed. New York (NY): McGraw-Hill; 1993.

Hamming R. Digital filters. 3rd ed. New York (NY): Dover Publications; 1997.

Hentschel T. Sample rate conversion in software configurable radios. Boston (MA): Artech House; 2002.

Pierce J. An introduction to information theory: symbols, signals, and noise. New York (NY): Dover Publications; 1980.

Soumekh M. Fourier array imaging. Englewood Cliffs (NJ): Prentice Hall; 1994.

Waggener W. Pulse code modulation system design, Boston (MA): Artech House; 1999.

1 (PDF)	DEFENSE TECHNICAL INFORMATION CTR DTIC OCA
2 (PDF)	DIRECTOR US ARMY RESEARCH LAB RDRL CIO L IMAL HRA MAIL & RECORDS MGMT
1 (PDF)	GOVT PRINTG OFC A MALHOTRA
1 (PDF)	DIR USARL RDRL CIH S P JUNGWIRTH